

**MAGNETIC SEPARATION AND ANALYSIS OF PRODUCTS  
OBTAINED FROM COAL-FIRED POWER PLANT FLY ASHES  
OF NIKOLA TESLA B (SERBIA)**

**Slavomír HREDZÁK<sup>#</sup>, Rudolf A. TOMANEC<sup>\*\*</sup>, Marek MATIK<sup>\*\*\*</sup>,  
Vladimír ŠEPELÁK<sup>\*\*\*\*</sup>, Miroslava VÁCLAVÍKOVÁ<sup>\*</sup>**

*\*Institute of Geotechnics, Slovak Academy of Sciences,  
Watsonova 45,043 53 Košice, Slovak Republic*

*\*\*Faculty of mining and geology, University of Belgrade,  
Džušina 7, 11000 Belgrade, Serbia*

*\*\*\*at this time Department of Physical Chemistry, Faculty of Sciences,  
Palacký University, tř. Svobody 26, 771 46 Olomouc, Czech Republic*

*\*\*\*\* at this time Institute of Physical and Theoretical Chemistry, Technical  
University of Braunschweig, Hans-Sommer Straße 10, D-38106  
Braunschweig, Germany*

*(Received 26.11.2006.; accepted 4.12.2006.)*

**Abstract**

*The contribution deals with high gradient magnetic separation (HGMS) of fly ash from thermal power plant Nikola Tesla B (Serbia). The lignite fly ash was subjected to wet grain size analysis, dry and wet HGMS at the magnetic field induction of 0.09 T. As to iron content in magnetic product, the best result has been achieved by wet HGMS under application of potato starch as an additive, namely 27.43 % of Fe comparing to 3.20 % of Fe in a feed. Consequently, products of classifying and magnetic separation were subjected to microscopy, SEM, XRD and Mössbauer spectroscopy. Quartz was found as a dominant mineral, which is accompanied by plagioclase, calcite, magnetite and hematite. Mullite, fayalite and mayenite can also occur in fly ash. Mössbauer spectroscopy confirmed, that 57.8 % of iron is bonded in magnetite and 27.6 % in hematite.*

**Key words:** *fly ash, high gradient magnetic separation, XRD.*

---

*# Corresponding author: hredzak@saske.sk*

## **1. Introduction**

In Serbia approximately 70 % of energy is obtained from coal [1]. From a total installed capacity in Serbia of 8,732 MW, thermal power plants (TPPs) represent 5,171 MW (excluding the heating plants with 353 MW), i.e. about of 59 % [2]. A total coal consumption is of 37,000,000 tones, a total ash production is 7,500,000 tones and the area of coal ash dumps occupies of 1,639 ha [1].

TPP Nikola Tesla A and B is a power plant complex with a total net capacity of 2,662 MW located on the right bank of the river Sava, approximately 40 km upstream from Belgrade, near the town of Obrenovac. By far the largest one in Serbia, the complex generates around 16 TWh annually, which covers almost half of Serbia's needs for electricity. The complex and two of its plants are named in honour of Nikola Tesla [2, 3]. These power plants use lignite with the heating value of 5,500-8,000 kJ/kg and the average ash content of 20% mined from the Kolubara-Tamnava coal basin as fuel. [3]. These two plants are producing between  $4.2$  and  $4.5 \times 10^6$  ton of coal ash per year [1].

TPP Nikola Tesla B is located between the villages of Skela and Ushce. There are two generation units with a total net capacity of 1,160 MW. These units belong to the biggest ones in the Balkan and the Europe, respectively. TPP Nikola Tesla B was first synchronised on March 11, 1983 [3, 4, 5]. The main technological system for electrical energy production was executed in blocks, on the principle of connecting the basic equipment: boiler – steam turbine – generator – transformer. Nikola Tesla B is connected via transmission line and the distribution plant 400 kV to the electrical power system and as the basic power station satisfies the needs of the Serbian consumers. The basic characteristics are as follows: total area of power station 108 ha; ash waste area 600 ha; total height of the boiler 137 m; total height of the chimney 280 m [4]. The pictures of the TPP Nikola Tesla B are illustrated in Fig. 1 and Fig. 2 [6, 7].

From the above mentioned facts it is obvious, that solid wastes coming from coal combustion are a big problem in Serbia. Besides the classical utilisation fields of coal combustion products, such as cement works, concrete and mortar in building, field engineering there are unconventional ways of their application there.

For instance fly ashes can be applied in sorption processes at water conditioning and flue gases cleaning, namely either directly without any treatment or after zeolitization, consisting in hydrothermal processing.

Moreover, grains of fly ash magnetic concentrates with sufficiently high value of magnetic susceptibility can serve as a carrier of substance with high sorption capacity, i.e. as a magnetic core of composed sorbents, which are separable in magnetic field.

Well, submitted contribution describes the possibilities of Fe-concentrate obtaining from lignitic fly ash in the HGMS process. The sample of fly ash from TPP Nikola Tesla B has been tested.



**Fig. 1.** TPP Nikola Tesla B – view through the Sava river [6]



**Fig. 2.** TPP Nikola Tesla B [7]

## 2. Techniques and methods

Firstly, the sample of lignitic fly ash was subjected to grain size analysis. The grain size analysis performed by dry and wet ways using standard laboratory sieves with given mesh size, namely 40, 80 and 160  $\mu\text{m}$ . Secondly, experiments on single-stage high gradient magnetic separation (HGMS) were performed on magnetic separator JONES. HGMS was carried out in a cassette located between separator poles. The cassette was equipped by ribbed plates for enhancement of magnetic field gradient. The induction of magnetic field “B” during the comparative HGMS tests was of 0.09 T.

Two basic ways of HGMS have been applied. The dry one was performed classically without any treatments and also with purification of magnetic product by air stream. Thus, the grains with the lowest values of magnetic susceptibility were removed into non-magnetic product. The wet one was realised in the first case without any additive and in the second one the surfactants, such as detergent and potato starch were added to water suspension of fly ash. The solids concentration in feed was of 100 g.L<sup>-1</sup>. The products of screening and separation were weighted and subjected to chemical analyses. Thus, mass yields, contents and recoveries of observed components were determined and calculated, respectively.

As to chemical analysis, generally, the AAS method (Spectr AA-30 Varian) was applied. But in the case of total iron in magnetic products, where its higher content expected, samples were analysed by titration. Combustible matter was determined as a loss on ignition at 900 °C.

The measurements of volume magnetic susceptibility “κ” of screening and HGMS products have been performed by means of the Kappabridge KLY-2 Geofyzika Brno, at the following condition: the magnetic field intensity of 300 A.m<sup>-1</sup>, the field homogeneity of 0.2 % and the frequency of 920 Hz.

The enrichment of Fe in magnetic products “τ<sub>Fe</sub>” was calculated as follows: Fe-content in magnetic product/Fe-content in feed, i.e. usually also referred to as β/α.

A selected sample of magnetic product was subjected to SEM analysis. Similarly, selected products of classifying and magnetic separation were subjected to XRD study by means of analyser DRON-UM1 under the following conditions: radiation CuKα, Ni-filter, voltage 30 kV, current 20 mA, the size of the steps of goniometer 2°/min.

To explain presence of Fe-bearing phases of magnetic product in more detail the Mössbauer spectroscopy was carried out. The room-temperature Mössbauer spectroscopy measurements were made in transmission geometry using a conventional spectrometer in a constant acceleration mode. A <sup>57</sup>Co/Rh gamma-ray source was used. The velocity scale was calibrated relative to <sup>57</sup>Fe in Rh. A proportional counter was used to detect the transmitted gamma-rays. Mössbauer spectral analysis software RECOIL [8] was used for the quantitative evaluation of the spectra. The spectra were fitted using the Voigt-based fitting method providing distributions of hyperfine parameters.

### 3. Chemical and grain size composition of lignitic fly ash

Chemical composition of individual grain size classes and calculated feed are presented in Table 1 and Table 3, respectively. Subsequently, recoveries of observed components into grain size classes are introduced in Table 2 and Table 4, respectively.

As to chemical composition the main components are represented by SiO<sub>2</sub> and Al<sub>2</sub>O<sub>3</sub>. A low content of combustible matter considers as a favourable property of this lignitic fly ash. From tabled data some dependencies can be also visible. For instance, contents of Al<sub>2</sub>O<sub>3</sub>, Fe and CaO increases with diminishing grain size, conversely, the content of SiO<sub>2</sub> fall down. Similar courses are possible to observe in case of recoveries. An irregularity at recovery of SiO<sub>2</sub> and Al<sub>2</sub>O<sub>3</sub> into a class of +160 μm is caused by the high mass yield of this class. Similar case is as to recovery of SiO<sub>2</sub> into class of 40 – 80 μm.

Finally, on the basis of results of this grain size analyses, it is difficult to determine one suitable cut of classifying to separate some utility component. Perhaps, two cuts can be considered, namely 40 and 160 μm, which enable to prepare pre-concentrates for following operations. Only combustible matter is pre-concentrated in the coarsest class.

**Table 1.** Chemical composition as a dependence of grain size – dry analysis

grain size [μm]	mass yield [%]	content [%]						volume magnetic susceptibility κ.10 <sup>-6</sup> SI unit
		combustible matter	SiO <sub>2</sub>	Al <sub>2</sub> O <sub>3</sub>	Fe	CaO	MgO	
+500	1.36	39.06	32.21	13.92	2.11	2.50	1.34	3,180.487
160 – 500	28.01	1.15	77.54	8.65	1.52	1.61	1.03	4,788.286
80 – 160	20.28	1.22	57.71	16.27	3.31	4.87	1.84	8,099.469
40 – 80	33.53	0.92	54.43	16.67	3.74	7.86	2.40	6,939.741
– 40	16.82	0.81	48.53	16.12	4.27	10.82	3.10	7,630.954
feed	100.00	1.55	60.27	14.21	3.10	5.93	2.01	6,947.310

**Table 2.** Recoveries of components into grain size classes – dry analysis

grain size [μm]	recovery [%]					
	combustible matter	SiO <sub>2</sub>	Al <sub>2</sub> O <sub>3</sub>	Fe	CaO	MgO
+500	34.45	0.73	1.34	0.93	0.58	0.91
160 – 500	20.82	36.03	17.06	13.74	7.60	14.35
80 – 160	15.99	19.42	23.21	21.67	16.66	18.59
40 – 80	19.94	30.28	39.32	40.48	44.47	40.16
– 40	8.81	13.54	19.08	23.19	30.69	25.99
feed	100.00	100.00	100.00	100.00	100.00	100.00

**Table 3.** Chemical composition as a dependence of grain size – wet analysis

grain size [μm]	mass yield [%]	content [%]						volume magnetic susceptibility κ.10 <sup>-6</sup> SI unit
		combustible matter	SiO <sub>2</sub>	Al <sub>2</sub> O <sub>3</sub>	Fe	CaO	MgO	
+ 160	32.78	2.43	76.13	10.05	1.87	1.93	1.16	5,019.76
80 – 160	17.67	1.34	60.40	16.70	3.57	4.59	1.97	8,739.72
40 – 80	22.75	1.26	57.32	17.33	3.63	6.66	2.26	6,856.32
– 40	26.80	3.16	47.73	17.50	4.72	10.98	2.95	8,199.95
feed	100.00	2.17	61.46	14.88	3.33	5.90	2.03	6,947.31

**Table 4.** Recoveries of components into grain size classes – wet analysis

grain size [μm]	recovery [%]					
	combustible matter	SiO <sub>2</sub>	Al <sub>2</sub> O <sub>3</sub>	Fe	CaO	MgO
+160	36.76	40.60	22.15	18.38	10.72	18.71
80 – 160	10.93	17.37	19.84	18.92	13.74	17.15
40 – 80	13.23	21.21	26.49	24.76	25.67	25.23
– 40	39.09	20.81	31.52	37.94	49.87	38.91
feed	100.00	100.00	100.00	100.00	100.00	100.00

#### 4. Results of HGMS tests

The results of HGMS tests are introduced in Table 5-10. The dry way of HGMS was not successful (Table 5-6). This fact partially expected on the basis of experiences, which were reported in [9, 10, 11]. The content and enrichment of Fe are low, similarly, the other parameters are also unfavourable.

Better results were obtained under application of wet way of HGMS. Iron content and its enrichment in magnetic products is much higher comparing to dry way, namely the content of Fe ranges from 21 to 27 % and the enrichment attain the values up to 8.5.

The magnetic products obtained by wet HGMS attain the values of magnetic susceptibility, which enables their removal in magnetic field, thus they can serve as a magnetic carrier for substances with high sorption capacity.

**Table 5.** Dry magnetic separation ( $\tau_{Fe} = 1.28$ )

product	mass yield [%]	content [%]					recovery [%]					magnetic susceptibility $\kappa \cdot 10^{-6}$ SI unit
		Fe	c.m.*	SiO <sub>2</sub>	Al <sub>2</sub> O <sub>3</sub>	CaO	Fe	c.m.*	SiO <sub>2</sub>	Al <sub>2</sub> O <sub>3</sub>	CaO	
magnetic	56.46	4.25	1.48	54.03	17.21	6.10	72.60	53.62	51.77	62.20	66.49	8,372.12
non-magnet.	43.54	2.08	1.66	65.29	13.57	3.99	27.40	46.38	48.23	37.80	33.51	2,506.43
feed	100	3.31	1.59	58.93	15.63	5.18	100	100	100	100	100	5,818.35

\*combustible matter

**Table 6.** Dry magnetic separation – magnetic product re-purified by air flow ( $\tau_{Fe} = 1.88$ )

product	mass yield [%]	content [%]					recovery [%]					magnetic susceptibility $\kappa \cdot 10^{-6}$ SI unit
		Fe	c.m.*	SiO <sub>2</sub>	Al <sub>2</sub> O <sub>3</sub>	CaO	Fe	c.m.*	SiO <sub>2</sub>	Al <sub>2</sub> O <sub>3</sub>	CaO	
magnetic	17.44	6.42	1.38	49.52	17.46	6.81	32.86	14.64	14.44	24.50	20.18	19,911.94
non-magnet.	82.56	2.77	1.70	61.96	15.13	4.44	67.14	85.36	85.56	75.50	79.82	3,664.90
feed	100	3.41	1.64	59.79	15.53	4.86	100	100	100	100	100	6,498.13

**Table 7.** Wet magnetic separation – water only ( $\tau_{Fe} = 7.84$ )

product	mass yield [%]	content [%]					recovery [%]					magnetic susceptibility $\kappa \cdot 10^{-6}$ SI unit
		Fe	c.m.*	SiO <sub>2</sub>	Al <sub>2</sub> O <sub>3</sub>	CaO	Fe	c.m.*	SiO <sub>2</sub>	Al <sub>2</sub> O <sub>3</sub>	CaO	
magnetic	1.97	27.11	1.45	29.23	12.00	8.76	15.46	1.44	0.99	1.43	3.58	120,779.29
non-magnet.	98.03	2.98	1.99	59.04	16.57	4.74	84.54	98.56	99.01	98.57	96.42	4,017.28
feed	100	3.46	1.98	58.45	16.48	4.83	100	100	100	100	100	6,317.84

**Table 8.** Wet magnetic separation with additive of detergent ( $\tau_{Fe} = 6.34$ )

product	mass yield [%]	content [%]					recovery [%]					magnetic susceptibility $\kappa \cdot 10^{-6}$ SI unit
		Fe	c.m.*	SiO <sub>2</sub>	Al <sub>2</sub> O <sub>3</sub>	CaO	Fe	c.m.*	SiO <sub>2</sub>	Al <sub>2</sub> O <sub>3</sub>	CaO	
magnetic	2.86	21.75	2.48	35.01	13.26	9.22	18.13	3.47	1.63	2.48	5.35	90,942.45
non-magnet.	97.14	2.89	2.03	62.09	15.34	4.80	81.87	96.53	98.37	97.52	94.65	4,159.06
feed	100	3.43	2.04	62.32	15.29	4.93	100	100	100	100	100	6,640.26

**Table 9.** Wet magnetic separation with additive of potato starch ( $\tau_{Fe} = 8.57$ )

product	mass yield [%]	content [%]					recovery [%]					magnetic susceptibility $\kappa \cdot 10^{-6}$ SI unit
		Fe	c.m.*	SiO <sub>2</sub>	Al <sub>2</sub> O <sub>3</sub>	CaO	Fe	c.m.*	SiO <sub>2</sub>	Al <sub>2</sub> O <sub>3</sub>	CaO	
magnetic	1.83	27.43	1.85	29.50	12.32	8.55	15.66	1.13	0.89	1.51	3.32	121,039.35
non-magnet.	98.17	2.75	3.02	60.99	14.93	4.63	84.34	98.87	99.11	98.49	96.68	4,342.90
Feed	100	3.20	3.00	60.41	14.87	4.70	100	100	100	100	100	6,475.88

**Table 10.** Wet magnetic separation with additive of the both detergent and potato starch ( $\tau_{Fe} = 7.97$ )

product	mass yield [%]	content [%]					recovery [%]					magnetic susceptibility $\kappa \cdot 10^{-6}$ SI unit
		Fe	c.m.*	SiO <sub>2</sub>	Al <sub>2</sub> O <sub>3</sub>	CaO	Fe	c.m.*	SiO <sub>2</sub>	Al <sub>2</sub> O <sub>3</sub>	CaO	
magnetic	2.10	26.14	1.99	29.64	12.13	8.62	16.74	1.21	1.02	1.68	3.90	116,074.81
non-magnet.	97.90	2.79	3.50	61.46	15.23	4.56	83.26	98.79	98.98	98.32	96.10	4,306.60
feed	100	3.28	3.47	60.79	15.17	4.65	100	100	100	100	100	6,654.26

### 5. Ore microscopic observation

The observations were performed by classical ore microscope “American Optical”. Results are introduced in Fig. 3.

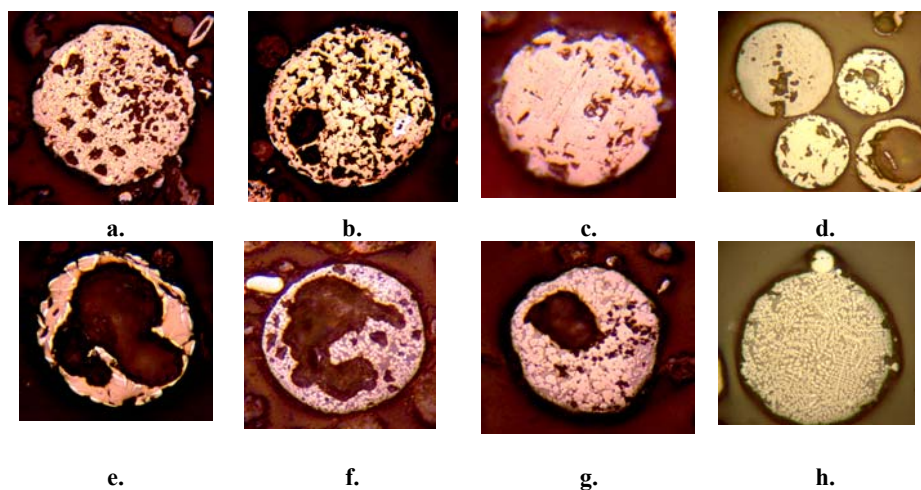


**Fig. 3.** Microphotographs of the polished sections of ferrospheres with different textural properties

**Legend:** a, b, g – glass basis with the mosaic-shaped structure of crystallites of complex Fe-oxides.; c, d – type of compact conosphere of ferrispinel (c) and expanded (e) with the skeletal and the textures of the solid solutions decay; f, g – expanded conospheres of ferrispinel, with the mosaic-shaped structure of crystallites of the complex Fe-oxides that builds only the “shell”; h – type of oriented intergrowth with the lines of ferrispinel crystallites in the glass matter.

## 6. SEM Analysis

SEM was performed for demonstration of magnetic particles morphology as it is illustrated in Fig. 4-5. Particles size ranges approximately from 5 to 70  $\mu\text{m}$ . They have a ball-like shape, which is often deformed, probably as a result of melting-down. The surface of them is rugged, better said broken and this fact can show itself in a higher value of specific surface.

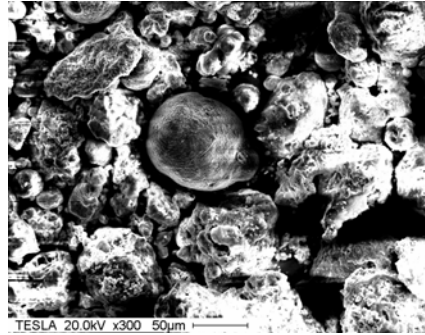


**Fig. 4** SEM pattern of magnetic product of fly ash

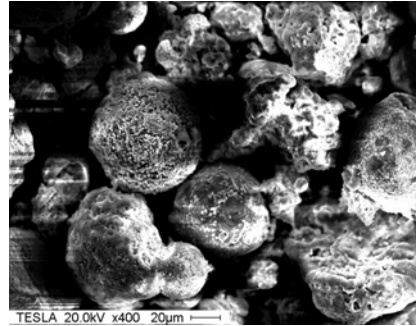


**Fig. 5** SEM pattern of magnetic product of fly ash

## 7. XRD study

XRD patterns of selected product of classifying and magnetic separation are introduced in Fig. 6. – 10.

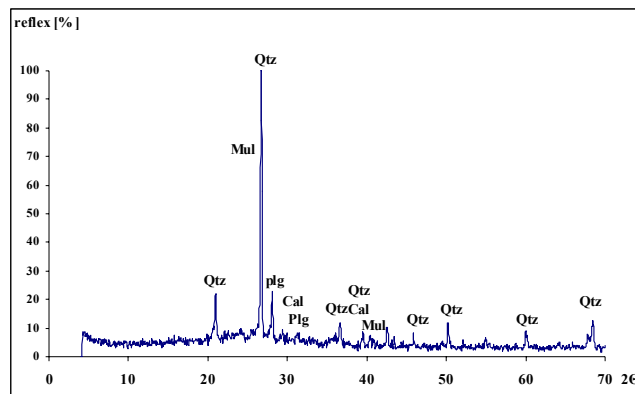


**Fig. 6.** Non-magnetic product

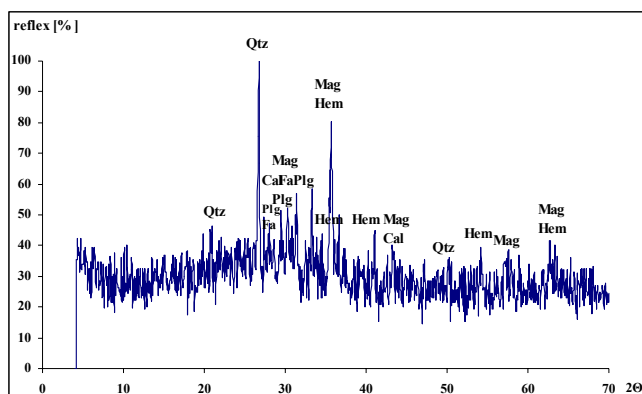


Fig. 7. Magnetic product

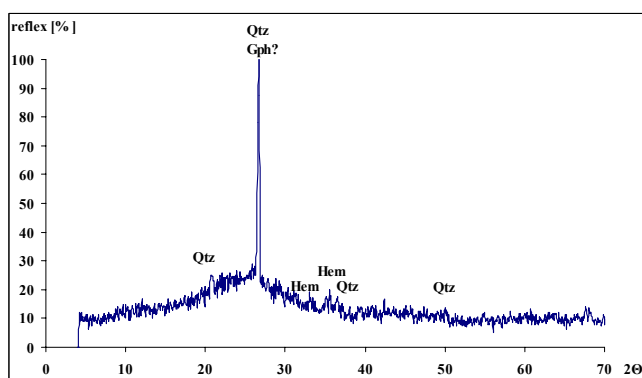


Fig. 8. XRD pattern +500 μm – dry classifying

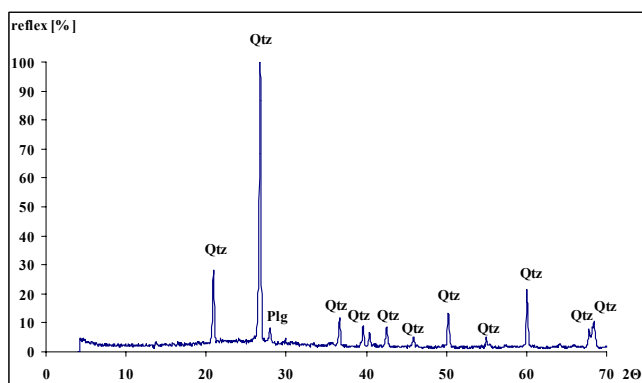
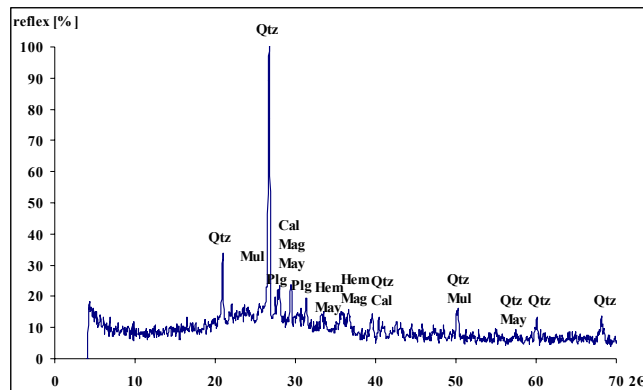


Fig. 9. XRD pattern +160 μm – wet classifying



**Fig. 10.** XRD pattern -40 μm – wet classifying

**Legend:** Qtz – quartz  $\text{SiO}_2$ , Plg – plagioclase (probably labradorite  $(\text{Ca},\text{Na})(\text{Si},\text{Al})_4\text{O}_8$ ), Cal – calcite  $\text{CaCO}_3$ , Mul – mullite  $\text{Al}_6\text{Si}_2\text{O}_{13}$ , May – mayenite  $\text{Ca}_{12}\text{Al}_{14}\text{O}_{33}$ , Mag – magnetite  $\text{Fe}_3\text{O}_4$ , Hem – hematite  $\alpha\text{-Fe}_2\text{O}_3$ , Fa – fayalite  $\text{Fe}_2\text{SiO}_4$ , Gph – graphite C.

Thus, quartz was identified as a dominant mineral in all patterns. Naturally, an higher occurrence of magnetite and hematite recorded in magnetic product of separation. As to the other Fe-bearing minerals fayalite can be present in this product

Accompanying minerals are generally represented above all by plagioclase and calcite. Some peaks indicates the presence of mullite and mayenite.

In the coarsest sample obtained by dry classifying an amorphous phase occurs probably as C-bearing component. The presence of graphite is uncertain.

For better illustration the chemical composition of analysed samples is summarised in Table 11.

**Table 11.** Chemical composition of XRD patterns

XRD pattern	c.m.	$\text{SiO}_2$	Fe	Al	Ca	Mg
non-magnetic product water-only	1.99	59.04	2.98	8.77	3.39	1.26
magnetic product water-only	1.45	29.23	27.11	6.35	6.26	1.59
+500μm dry classifying	39.06	32.21	2.11	7.37	1.79	0.81
+160 μm wet classifying	2.43	76.13	1.87	5.32	1.38	0.70
-40μm wet classifying	3.16	47.73	4.72	9.26	7.85	1.78

## 8. Mössbauer spectroscopy

The Mössbauer spectrum of obtained magnetic product is illustrated in Fig. 11. Description of iron state summarised in Table 12. Thus, as to Fe-bearing minerals magnetite is dominant and it is accompanied by hematite. An occurrence of superparamagnetic and paramagnetic more closely unspecified phases was detected.

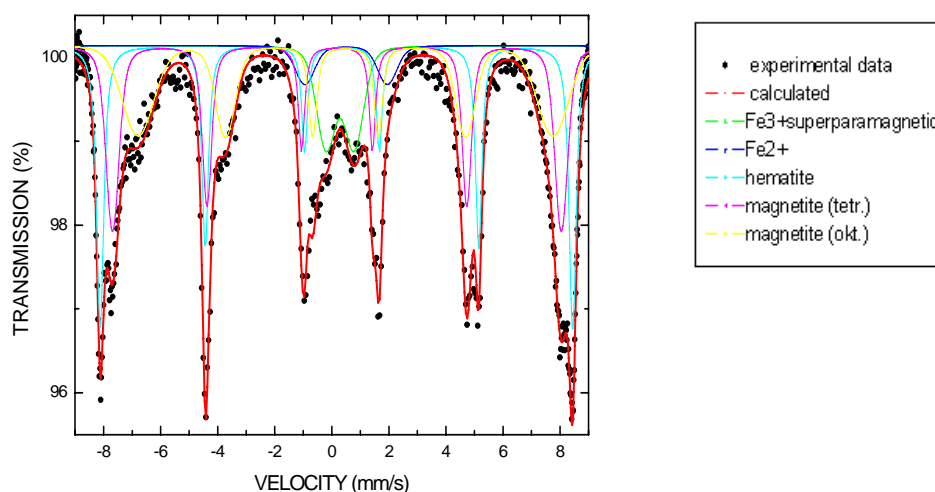


**Fig. 11.** Mössbauer spectrum of magnetic product

**Table 12.** Description of iron state

Oxidation state of iron	Magnetic state of iron	wt %
Fe <sup>2+</sup> ; Fe <sup>3+</sup>	magnetically ordered in Fe <sub>3</sub> O <sub>4</sub>	57.8
Fe <sup>3+</sup>	magnetically ordered in $\alpha$ -Fe <sub>2</sub> O <sub>3</sub>	27.6
Fe <sup>3+</sup>	superparamagnetic	10.5
Fe <sup>2+</sup>	paramagnetic in a Fe <sup>2+</sup> -containing phase	4.1

## 8. Conclusion

The submitted contribution was focused on obtaining of Fe-spherules in the process of high gradient magnetic separation (HGMS).

Obtained results point to fact, which wet way of HGMS seems to be favourable for preparation of Fe-concentrates. It was proven, that magnetic product of approx. 27 % Fe can be won under application of potato starch as

an additive to feed. The magnetic susceptibility in such way prepared Fe-concentrates, i.e.  $90 - 120 \cdot 10^{-3}$  SI units, enables their utilization as magnetic core of composed sorbents.

From economical point of view, it needed to mention that mass yield is low (up to about 2%). For this reason magnetic separation of all grain size scale is not real. But at concern about such product on market it possible to consider cheaper pre-treatment, for instance classifying with a cut ( $d_{50}$ ) between of  $40 - 80 \mu\text{m}$  or gravity pre-concentration.

XRD study confirmed that quartz is dominant mineral of fly ash. It is accompanied by plagioclase, calcite, magnetite and hematite. Mullite, fayalite and mayenite can also occur. Mössbauer spectroscopy showed that 57.8 % of iron is bonded in magnetite and 27.6 % in hematite.

## **10. Acknowledgements**

The presented work was supported by Slovak grant agency for the VEGA projects No. 2/5146/25 and 2/5150/25, Bilateral Scientific and Technological Cooperation between Serbia & Montenegro and Slovakia under the project „Complex Processing and Utilization of Fly Ashes from Coal-Fired Power Plants“ and the Task of the State Program No. 2004 SP 26 028 0C 01 “High Tech and New Technologies for the field of obtaining and processing of industrial minerals”.

## **11. References**

1. A. Popovic, B. Adnadjevic, D. Djordjevic, P. Polic, "Coal ash – speciation of microelements, pollution potential and possibilities of usage",  
(<http://www.ucis.pitt.edu/global/gap/environmental/presentations/Popovic.pdf>,  
<http://www.ucis.pitt.edu/global/gap/environmental/files/Popovic.pdf>).
2. Electric Power industry of Serbia, Annual Report 2005, Publikum Beograd, (2005), [www.eps.co.yu](http://www.eps.co.yu).
3. [http://en.wikipedia.org/wiki/TPP\\_Nikola\\_Tesla](http://en.wikipedia.org/wiki/TPP_Nikola_Tesla)
4. <http://www.yu-build.com/main/i/095/095.html>
5. [http://www.eps.co.yu/onama/tpp\\_ntesla\\_b.htm](http://www.eps.co.yu/onama/tpp_ntesla_b.htm)
6. <http://www.yu-build.com/main/i/095/095a.html>

7. <http://www.eps.co.yu/zaposetioce/galerija/tent/tentb01.jpg>
8. K. Lagarec, D.G. Rancourt, "RECOIL - Mössbauer Spectral Analysis Software for Windows, version 1.02", Department of Physics, University of Ottawa, Ottawa, (1998).
9. S. Hredzak, M. Vaclavíkova, S. Jakabsky, M. Lovas, M. Matik, "Treatability of ash from coal-fired power plant EVO1 by magnetic way", In: Proc. of the 7<sup>th</sup> Conference on Environment and Mineral Processing - Part II. (ed. Peter Fecko) - VŠB-TU Ostrava, pp. 85 – 89, (2003).
10. S. Hredzak, S. Jakabsky, M. Lovas, M. Vaclavikova, M. Matik, "Selected results of the research on fly ashes wet magnetic separation", In: Zbornik XIX Srpsko Crnogorski Simpozijum o Pripremi Mineralnih Sirovina, Izdavač: Komitet za PMS, Institut za tehnologiju nuklearnih i drugih mineralnih sirovina, Beograd, Topola – Oplenac, pp. 67 – 73, (2004).
11. S. Hredzak, S. Jakabsky, M. Vaclavikova, J. Kurucz, "Magnetic separation of ash from the Heating plant of Kosice", In: Proc. of the 8<sup>th</sup> Conference on Environment and Mineral Processing, Part II. (eds. Peter Fecko & Vladimir Cablík), VŠB-TU Ostrava, pp. 257 – 260, (2004).